DopSCA, Scatterometer-based Simultaneous Ocean Vector Current and Wind Estimation

Hoogeboom, Peter; Stoffelen, Ad; Lopez Dekker, Paco

DOI
10.1109/DOfS.2018.8587276

Publication date
2018

Document Version
Accepted author manuscript

Published in
Proceedings of the Doppler Oceanography from Space

DopSCA, Scatterometer-based Simultaneous Ocean Vector Current and Wind Estimation

Peter Hoogeboom
Department of Geoscience and Remote Sensing
Delft University of Technology
Delft, Netherlands
p.hoogeboom@tudelft.nl

Ad Stoffelen
Active Remote Sensing Group, Satellite R & D
Royal Netherlands Meteorological Institute
de Bilt, Netherlands
ad.stoffelen@knmi.nl

Paco Lopez-Dekker
Department of Geoscience and Remote Sensing
Delft University of Technology
Delft, Netherlands
F.LopezDekker@tudelft.nl

***Abstract*— Satellite wind scatterometers like the MetOp SG (Second Generation) SCA of Eumetsat are not designed to measure ocean currents, yet if they could, it would improve the wind vector product and provide important additional information to the oceanographic community for various applications. Previous publications showed this possibility, but only with modifications to the system. In this paper the possibilities of measuring the ocean current vector simultaneously with the wind vector without modifications to the SCA system, are investigated through simulation studies. The measurement principle relies on phase change in a pulse pair measurement. The results indicate that it should be possible with SCA to measure the ocean current vector simultaneously with the wind with an accuracy of better than 1 m/s on a 50 x 50 km grid.**

Keywords— satellite radar, ocean current, wind scatterometer, Doppler measurement

I. INTRODUCTION

A. Background

Dedicated radar missions to retrieve ocean currents are still in development. An example of a system under study is Wavemill [8]. Another promising instrument is SKIM, the Sea-surface Kinematics Multiscale monitoring instrument [1, 10], a candidate for ESA's Earth Explorer 9. It would carry a novel wide-swath scanning multi-beam radar altimeter to measure ocean-surface currents by a Doppler technique. Such dedicated instruments promise to deliver high precision ocean current measurements, fulfilling most of the requirements in the oceanographic community. However such instruments are expensive and require a long development time. Meanwhile indirect methods, using radar altimeters and wind scatterometers are frequently used, which provide us with global and regional maps of the ocean surface's mesoscale motion on scales larger than 100 km [3]. Obtaining ocean current information on scales of 50 km and smaller thus remains a challenge. The definition of ocean current is part of the challenge.

DOPSCAT was a study into the capabilities of a satellite wind scatterometer to retrieve ocean currents. The future MetOp SG (Second Generation) SCA instrument of Eumetsat (to be launched in 2021) served as design guide [2, 17]. It soon proved impossible to meet the demanding requirements in ocean current determination. However with special waveforms and some system modifications it was deemed possible to attain 0.2 – 0.3 m/s minimum current sensitivity. The study resulted in a number of papers, a PhD-thesis and recommendations for adaptations to the SCA instrument on the METOP SG platform [4-6].

Investigations by the instrument provider Airbus revealed on one hand that the assumed adaptations on the instrument were not feasible or compatible with time and budget constraints, while on the other hand the simulation results were inconsistent with certain radar theories [12]. Apparently the simulations were not accurate or complete enough to reveal this. In a meeting with several parties the details were discussed [13]. This formed the basis for a new investigation which is reported in this paper.

B. Problem statement

The problem at hand is to measure Doppler shift with the antennas and radar hardware of a space-borne wind scatterometer. In principle the Metop SCA instrument will be fully coherent and can be used to measure Doppler. This instrument will have three antennas on either side, pointing at 45, 0 and -45 degrees azimuth with respect to the normal on the velocity vector in the horizontal plane. The two times three antennas will cover each a swath of around 660 km, where the corresponding incidence angles range from 20 to 65 degrees. The antenna size in elevation must be small to cover this angular range. In azimuth (flight direction) the antennas will measure some 3 to 4 meter. The platform will travel at 6.8 km/s. The radar PRF will be quite low, in the order of 32 Hz. The pulses are to be used sequentially on the six antennas, so per antenna the PRF is even lower.

These parameters are perfectly suited for the wind vector measurement and compliant with the range ambiguity requirement. However, to measure small Doppler shifts with these parameters is impossible. An ocean current of 1 m/s at C-band (5.4 GHz) results in less than 40 Hz Doppler shift. The only possibility to measure Doppler is to make use of a coherent measurement interval, which has an approximate duration given by the time the antenna travels half an antenna length, after which the coherence drops significantly. A pulse pair waveform could be used to measure phase shift in this short interval. Since its duration is in the order of 0.25 ms, a low Doppler sensitivity (in the order of 400 Hz) can be expected, too small to find ocean current in a single measurement. The wind scatterometer will have a relatively high range resolution in the order of 150 meter. Independent range resolution cells are used for speckle reduction by averaging, to produce wind vector measurements with high accuracy over larger areas of 25 x 25 km or 50 x 50 km) This

approach would also allow for immense averaging over up to 10,000 independent samples for Doppler measurements, leading to acceptable performance, if the range ambiguities stemming from the short time between the pulses in the pulse pair can be avoided.

C. Doppler measurement and ocean motion

In this paper the Doppler estimation of ocean current with the SCA instrument has been further studied. SCA is designed to make wind scatterometer measurements with a sequence of 8 pulses, 6 of which are dedicated to the 6 antennas, 2 are freely configurable without sacrificing performance on the wind vector product. One application is a cross polarization measurement in case of high wind speeds, to improve the accuracy of the wind measurement. But another could be to measure the ocean motion (the Stokes drift, related to the local wind), knowledge of which also improves the wind retrieval. With two pulses on the + and – 45 deg. antennas the ocean motion vector could be measured on one side of the spacecraft. A new and original Doppler-centroid retrieval method has been developed, which overcomes the problem of range ambiguities. Some basic simulations have been performed. One remaining issue that affects the accuracy of a Doppler mode is the pointing accuracy of the instrument. While ideas exist on methods to improve the pointing in post-processing, this approach would need further consolidation and a proper performance assessment and is not addressed in this paper.

Note that we distinguish ocean motion and ocean current, where the latter refers to the mean water movement of the ocean surface, but the former also includes the "net" motion of ocean waves and drifts [11] as seen in the SCA geometry. As is well understood, a large part of the geophysical Doppler measured by a radar is due to a so-called wave bias. This wave bias is caused by the correlation between the local slopes, which modulate the backscattering, and the corresponding local orbital velocities, which result in local Doppler signatures. Most of this bias is associated to wind-induced waves with wavelengths in the order of 10 m and has been empirically modelled using SAR [9]. Therefore, this wave bias is also often referred to a wind bias, and it needs to be jointly estimated with the surface current. Since ocean motion, and thus Doppler, depends on the local wind and waves, it is a prerequisite to measure accurate local wind information to be able to retrieve accurate ocean currents. The SCA instrument would thus be well suited from this perspective to obtain ocean current.

D. Paper organization

The paper is organized as follows: in chapter 2 the observed Doppler shift from an ocean surface is discussed for the case of a moving antenna. Chapter 3 is about the new double pulse observation method to detect ocean Doppler without range ambiguities. Chapter 4 discusses the setup of the numerical simulation software, which was developed in Python. Chapter 5 reviews the results and chapter 6 is the conclusion.

II. Representation of Doppler shift from an ocean surface, employing a moving antenna

A. A simple scatter model

In this phase of the study it is essential to have a simple but correct radar model of the response of an ocean surface that is illuminated with a moving radar antenna. It is for now less important to have a detailed ocean scatter model. Our first interest goes to the phase response. To simplify matters most of the amplitude factors are neglected. It is important to describe the surface with a large enough number of scatterers in a resolution cell, and to cover a large area, consisting of many resolution cells (the SCA range resolution is approximately 150 m). In particular the surface has to be considered as a distributed target. Each scatterer is characterized by its position, its speed and direction of motion, its microwave phase jump on reflection and its strength. The latter two are neglected, we have assumed equal reflection strength and phase jump for all scatterers.

The antenna performs a vectorial addition on the contributions from all the scatterers. For a stationary antenna it would be possible to measure phase changes from a scene over a relatively long period, say the scene decorrelation time of the surface, which is in the order of milliseconds in the case of an ocean surface. But when the antenna moves, the phase of each scatterer changes according to its position in the resolution cell, resulting in a rapidly changing phase at the output of the antenna.

It can be shown that an antenna displacement over half a wavelength reshuffles the vectorial addition over all scatterers over 2π, resulting in a more or less independent phase at the new antenna position. Note that each range resolution cell in an image of distributed targets will present a random phase value.

B. Doppler bandwidth of moving antenna signal

Next we consider the bandwidth of the received signal in a moving antenna. For a completely filled beam, the Doppler bandwidth B is dependent on the antenna beam width β, antenna speed v, antenna look angle θ (for SCA θ can be 0, ±45 deg.) with respect to cross-track direction and the wavelength λ, see the formula in fig. 1. Note that for $\theta = 0$ and for small β this relation reduces to the well-known equation used in SAR analysis. Since the scatterers have random positions within the resolution cell, the sum response exhibits a randomly varying amplitude and phase (assuming there are many scatterers in a resolution cell), that is to say on a short time scale the output signal samples of the antenna are coherent, but at longer time scales the signal samples lose their coherence. This property of the signal is described by the decorrelation time, which equals to approximately $1/B$.

Despite the varying phase as described above, it is expected that after a short time the phase output of the antenna will contain an additional small, solid phase shift if all the scatterers have a speed component in the direction of the radar, which is a reasonable assumption for a homogeneous ocean surface. This small solid phase shift can be retrieved, if the random phase variation due to the antenna motion over the measurement time is small enough. A phase signal randomly

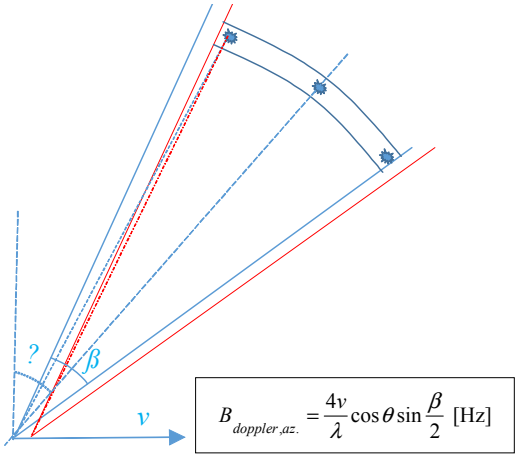

Figure 1: Doppler bandwidth of the received signal in a moving antenna for squinted observation.

distributed over 2π has a standard deviation of π/√3. In that case a small phase variation added to the random signal is lost. In our approach the time between the measurements is chosen short enough to keep the phase variation due to decorrelation well below π/√3, see fig. 4 for an example, and therefore it is possible to retrieve the small phase shift in an averaging procedure. Note that in all these cases we are dealing with pulsed observations, and the phases are found as phase changes from the pulse pairs.

C. *Constraints*

A few constraints arises here: from Doppler point of view, it would be worthwhile to have sufficient time between two pulses, but from antenna motion point of view the time between the pulses has to be short because of the decorrelation property of the moving antenna. Furthermore, for a single resolution cell the responses of the cell to the two pulses have to be separated, which is usually done for point targets with orthogonal waveforms. In that situation the only other requirement is, as is well-known from SAR systems theory [14], that the range covered by the antenna is sufficiently short to avoid ambiguities. This is contradictory to the large range observation requirement of the wind scatterometer [15]. In addition, to make things worse: for distributed targets orthogonality of waveforms has no effect. Rather than focusing the energy as is the case with a point target for one waveform and smearing it out for the orthogonal one, in the case of distributed targets the energy of both waveforms is more or less evenly redistributed over the resolution cells, resulting in a Signal to Clutter Ratio (SCR) of 1. Of course that impacts the phase measurement.

Two more factors influence the phase at the output of the radar system: the look direction θ (orientation in azimuth, see fig. 1) and the motion of the antenna during the transmission of a (long) pulse both introduce Doppler shifts. The Doppler component in the received signal due to the antenna motion depends on the speed v of the antenna and the wavelength λ. This component can be easily corrected. A correction for the look direction is also fairly easy, except that the required precision becomes very high, if the residual Doppler has to be very small. The pointing accuracy of the platform plays an important role. This has not been part of the current study.

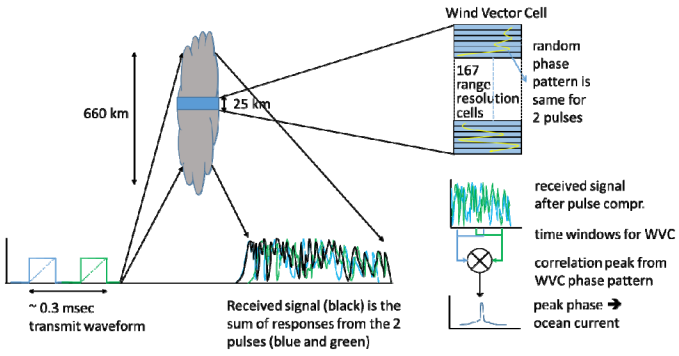

Figure 2: Observation schematic for ocean current retrieval.

III. NEW APPROACH TO THE DOPPLER MEASUREMENT

To overcome the aforementioned problems and controversies, in fig. 2 a new approach is outlined, which makes use of two well-known radar techniques:
- Pulse Pair Processing, as often used in weather radar [7] to obtain an average speed from a volume of raindrops, and
- Noise radar [16], radar systems employing (pseudo-) noise waveforms. In noise radar systems the received signal from a scene is correlated with the transmitted noise waveform. The correlator achieves good range resolution and suppresses range ambiguities.

A. *Pulse pair observation*

Fig. 2 shows a transmit pulse pair, consisting of 2 chirps, which are transmitted in a short time window, less than 0.3 ms. This short time is required in the case of SCA due to the moving antenna decorrelation time, as already discussed. The two responses from any resolution cell will exhibit a phase difference corresponding to the Doppler shift of the ocean motion in that cell. However, the system setup results in a single output signal (in black in fig. 2), which is the sum of the two (blue and green) responses. The black aggregated signal is pulse compressed with the reference functions for the blue and the green transmit pulse. The reference functions are slightly different, because they include a phase correction for the change in antenna position between the two pulses. In the blue and green pulse compressor outputs, time windows for a WVC are selected. The green time window is created from the blue one, shifted by the delay between the blue and the green pulse. Hence two channels with the phase information of interest are created.

After pulse compression the SCA radar has 150 meter range resolution cells, whereby the wind scatterometer observes 25 km wide Wind Vector Cells (WVC) in a large swath (some 660 km) over the ocean. The actual radar range resolution is chosen this high to enable the reduction of

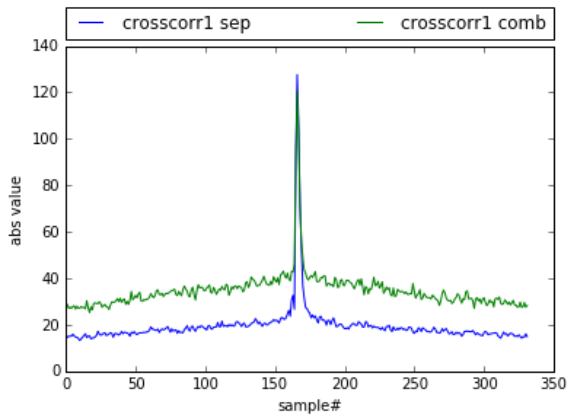

Figure 3: Cross correlation between the responses in a single WVC from the two pulses of a pulse pair after pulse compression. The blue line is a theoretical case, where the complete range responses of the two pulses are fully separated. The green line shows the realistic case of combined signals, including disturbance from neighbouring cells, whose reflection from one of the pulses coincide with the reflections of the cells under test. The peak to background ratio is therefore reduced.

speckle, the multiplicative noise in the radar measurements [14].[1]

B. Pulse pair phase observation

At this point one could try to measure the phase difference between coinciding resolution cells, but the resulting phase differences will show a very large variance. This is because the pulse compressed signals are contaminated by the influence of neighboring cells, for which the reflections coincide with one of the two pulses over the resolution cell of interest. This can be seen in fig. 2. The first (blue) and second (green) transmit pulses are separated by 0.2 ms or 30 km. The measurement of the 25 km WVC with the first pulse coincides with the response from the second pulse of an area 30 km closer to the radar. During the measurement of the WVC with the second pulse, an area 30 km further away from the radar presents its scatter at the same time. Consequently the black sum signal from the WVC contains responses from 3 x 25 km = 75 km ocean surface. Note that the use of orthogonal waveforms for the two pulses would not suppress the ambiguities. As already explained, the pulse compression of the random signals of a distributed target, is again random: the energy from the other pulse will simply be evenly distributed over the resolution cells, no matter the orthogonality of the waveform.

[1] It is important in the wind vector application to reduce the standard deviation of the backscatter measurements to find accurate wind vector values. According to the central limit theorem, averaging of N received echoes results in a speckle noise reduction of √N, if they are statistically independent, which is usually the case for range resolution cells. In flight direction the statistically independent results from M radar pulses can be added to the averaging procedure. The standard deviation is thus reduced by a factor √NM.
In case of SCA the WVC measures 25 x 25 km. In range the WVC has 25 km / 150 meter = 167 resolution cells. About 15 pulses are transmitted in a beam while the scatterometer travels over 25 km. In total the speckle reduction for a WVC is approximately 50 (2500 looks). For a 50 x 50 km WVC the reduction factor increases to nearly 100 (10000 looks).

C. Noise radar correlation technique

In order to extract the best possible phase difference from the pulse pair, the influence of these ambiguities is suppressed by applying the noise radar correlation technique. The high range resolution of the SCA is very helpful for the noise radar approach. Based on the discussion in chapter II.*A.* it is clear that every pixel produces a random phase value in response to a radar pulse. Accordingly the 167 consecutive range cells of the 25 km WVC cell appear as a pseudo-noise waveform, time shifted in the pulse pair response. Rather than averaging the detected signal (which discards the phase) as is done in the wind retrieval or calculating phase difference per resolution cell, the two (blue and green) time windows are correlated with each other to give a correlation peak for the pseudo noise pattern. The green plot in fig. 3 gives an example. A correlation peak will only occur if the random phase patterns from the two windows are the same. If there is too much delay between the pulses, or if the pulses are too long, the range cells will decorrelate and the correlation peak will decrease in value to eventually disappear. The phase of the correlation peak corresponds to the mean ocean motion of the WVC under investigation. Generally a mean motion exists due to waves, drifts and currents.

The responses of neighboring resolution cells as indicated in fig. 2 introduce deviations from the unique phase pattern, thereby introducing a higher noise level in the correlation plot, reducing the correlation peak and decreasing the accuracy of the phase measurement. The blue line in fig. 3 shows a result if the ambiguities could be fully suppressed. It is created by keeping the responses of the blue and the green pulse completely separated in the simulation calculations. The lower, but not zero, noise level for this case is due to the decorrelation introduced by the motion of the antenna and cannot be avoided.

Fig. 4 shows the cross correlation peak phase for 128 statistically independent runs. The phase value has considerable variance, but well below $\pi/4$, meaning that averaging over a number of realizations to reduce the variance is useful. The Cramér-Rao bound can be used to determine the

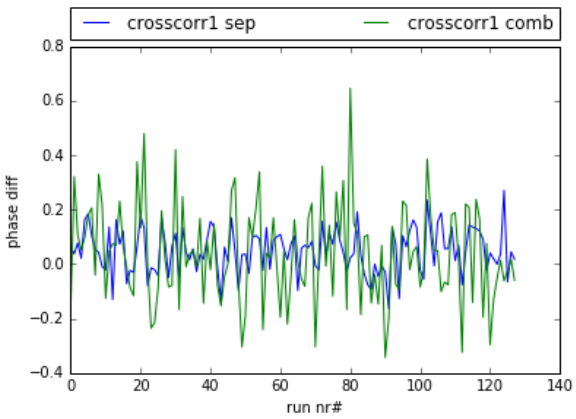

Figure 4: Cross correlation peak phase for 128 consecutive runs. Considerable averaging is required to reduce the phase noise. Again, the green line is the realistic case with combined responses from the two pulses in the pulse pair. The blue line shows the smaller phase noise level in the theoretical case of fully separated signals.

best possible accuracy of the ocean current estimation [15]:

$$\sigma_{vr}^2 = \left(\frac{1}{2k\tau_B}\right)^2 \frac{1}{2N_L}\frac{1-\gamma^2}{\gamma^2} \quad (1)$$

with:
σ_{vr} = the range velocity accuracy
k = the wavenumber
τ_B = time between two pulses
N_L = the number of looks
γ = the coherence

The number of looks was already found in footnote 1, 2500 for a 25 x 25 km WVC and 10,000 for a 50 x 50 km WVC. The coherence found with the later described simulation software is 0.41. Consequently the Cramér-Rao bound indicates a best ocean speed accuracy of 0.61 m/s for the 50 x 50 km WVC. This is in range direction. Due to the ground projection the actual result on the surface will be in the order of 0.85 m/s.

For phase measurement between two pulses it is advantageous if the two pulse waveforms are identical, but point like targets, could give rise to ambiguities, which cannot be resolved. Consequently, if the point target strengths are large compared to the ocean backscatter values, the phase measurement could be biased or disturbed. It is assumed that most of the wind scatterometer observations do not include point targets. However if it was the case, the use of chirps with slightly different chirp rates could be applied. Such a waveform will lead to a defocusing of the point target for the second pulse response if the data is convolved with the first reference function and vice versa. The defocused energy will increase the background clutter and thereby decrease the accuracy of the measurement, but not as strong as would be the case with a well-focused response for both pulses.

IV. NUMERICAL SIMULATION SETUP

A. Introduction

A numerical simulation program is set up in Python. The simulation is concerned with amplitude and phase of the radar video signal, as presented by the I and Q channels after mixing to zero carrier frequency. Particular care has been taken to implement correctly the influence of antenna motion and the presence of many scatterers. The radar representation of the ocean surface on a short time scale is a distributed target, with many scatterers, moving with some ensemble speed, that are observed from a moving antenna. Hence, the construction of the received signal in the antenna is complicated. Moreover, the distance between antenna and scatterers is large; in the time between transmission and reception the antenna moves more than 40 meter. Over the duration of the pulse pair waveform the antenna moves 2 meter, or more than 30 wavelengths. For the sake of clarity and precision the radar reflection calculations are performed in time domain.

In the simulation, scatterers are randomly placed in the resolution cells of the antenna beams with azimuth angles θ = + or -45 degrees. In the radar system the received signal is digitally sampled. Likewise the transmitted waveform consists of samples which are digitally generated. Synchronous sampling of receiver and transmitter is assumed. For each receive sample the contributions of all scatterers are accumulated, taking the exact delay time between transmission and reception for each scatterer into account. Based on the delay time the nearest transmit sample is chosen and hence the proper phase contribution per scatterer is found.

All instrument parameters have been selected within the operating boundaries of the SCA and without compromising the wind scatterometer application. The two spare pulses out of the sequence of eight are foreseen for the Doppler measurement, allowing ocean vector motion retrieval if the + and – 45 degrees antennas are used. The program does not include specific radar formula calculations or SNR calculations. It is assumed that the clutter of the second pulse is dominant over thermal noise.

B. Flow diagram

The flow diagram of the simulation program (see fig. 5) starts with defining a waveform {1} that may consist of 1 or 2 short pulses, each with its own programmable linear frequency chirp. The transmit chirp and the reference chirp (for convolution after reception) are generated separately. The reference chirp includes a Doppler correction, due to the speed of the spacecraft and due to the azimuth look angle of the beam.

The chirp bandwidth is adjustable, a maximum of 1 MHz has been used. Throughout the simulation program a 2 MHz sampling frequency with complex (I and Q) samples has been used. The maximum waveform length is 1.15 ms.

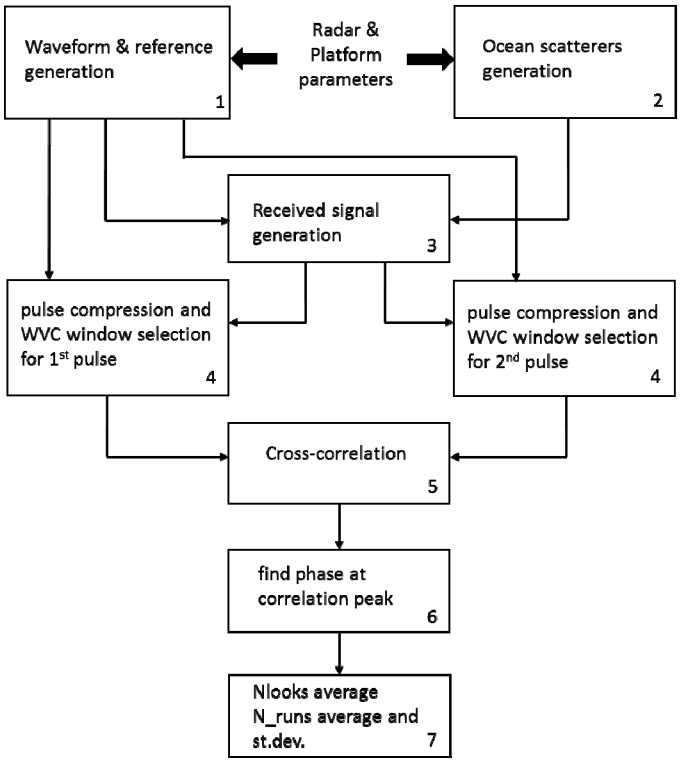

Figure 5: Flow diagram and functional blocks of the numerical simulation. Two pulses can be combined in a single wave form.

Next {2} an area on the ground is randomly filled with scatterers of equal strength. The scatterers are assumed to have all the same ocean motion vector. Although in reality the scatterers will have a spectrum of ocean motion, it is assumed here that the averaging procedures will result in a mean value. The center of the illuminated area on the ground is located at an adjustable distance, 1050 km is chosen here. The range is set equal to the length of the waveform plus the length of the WVC. Depending on the waveform length, values range from approximately 95 km to 140 km. At 150 m (1 MHz bandwidth) resolution the range spans some 700 to 900 range cells. The width of the illuminated area corresponds to the antenna beam width, about 18 km. The minimum number of scatterers per resolution cell is selectable in the program. A minimum value of 7 is chosen, which leads to between 4500 and 7000 scatterers in a single simulation. This number proved to be adequate in generating reliable statistics for a single simulation.

Next {3}, for each time sample of the pulses in the waveform (2 MHz sampling up to 1.15 ms yields maximally 2300 samples, of which only a part is used due to the upper limit of the antenna decorrelation time) the complex response for each scatterer is accumulated in a received signal array. In order not to sacrifice phase accuracy an analytic expression for the exact range between the antenna's transmit and receive position for a given scatterer was introduced, rather than the more usual approximation that the transmission and reception occur from a common, central point, in between the positions of transmit and receive. This approach includes determination of the exact position of the scatterer at the time it is hit by the pulse. In addition to a fully accumulated received signal array, the responses of the pulses in the waveform are also stored in separate received signal arrays. This was done to enable a results comparison with a situation where we would be able to separate the responses of the pulses, like it was anticipated in previous studies [4-6]. Fois used a down-chirp and an up-chirp along with a Separation Compression Filter. This approach will not be successful in the case of a moving antenna, as could be demonstrated with the simulation software from this study (not further discussed in this paper). Other approaches that would make the separate signal results applicable (e.g. a different radar system setup or signal suppression and separation) could be topics for future studies.

Next {4} the received signal is convolved with the reference functions belonging to the transmitted chirps. For each pulse the samples corresponding to the WVC of interest are selected after the pulse compression. The length of these arrays is one WVC (25 km), in samples 333. This value is also adjustable in the program.

The pulse pair responses are correlated {5} with each other in the next step. A peak will occur in the cross correlation if the unique phase pattern of the range cells in the WVC does not change too much over the time between pulses. The phase of the peak response {6} represents the mean ocean line-of-sight (LOS) component motion.

The processes {2 – 6} are repeated Nlooks times {7}. The phases of these Nlooks are averaged. For each look a new, independent random ocean scene is generated.

Table 1: Selected simulation parameters.

Radar instrument and platform			
Radar frequency:	5.4 GHz	Platform speed:	6800 m/s
Antenna length:	3.2 m	Range to WVC:	1050 km
Azimuth direction:	45 deg. (Fwd beam)	Footprint dimensions:	Approx. 18 km in azimuth 95 – 140 km in range (depending on waveform length)
Chirp bandwidth:	1 MHz max	Sample frequency:	2 MHz complex
Waveform length:	1.15 ms (max)	Pulse length:	0.115 ms
Nr. of pulses in waveform:	2	Delay between pulses:	0.115 (juxta-posted) to 0.23 ms
FM chirps:	up-up		
Analysis parameters			
Number of range samples in a WVC (25*25 km):	333	Number of looks in a WVC (25*25 km):	16 (could be twice as large if both spare pulses are used)
Simulated ocean currents:	0 & 3 m/s	Direction of ocean current:	225 deg.
Number of scatterers per resolution cell:	> 7	Number of scatterers in footprint:	4500 – 7000, depending on waveform length
Number of runs per case:	64		

Finally, data are stored from a sufficiently large number of runs (N_runs), leading to N_runs average phase values (on Nlooks), from which a reliable mean and standard deviation can be calculated. The accuracy of the measured ocean LOS motion component can be found from the average phase difference between two ocean LOS components (i.e. 0 and 3 m/s) and the standard deviation.

V. NUMERICAL SIMULATION RESULTS

It is important to use realistic platform and instrument parameters in the simulations. Information provided by Airbus [12] and ESA [17] was used to choose the parameters. Table 1 presents the selected values for the simulation runs.

The required footprint in the simulations is quite large. This ensures realistic clutter levels in every point of the WVC due to the extended pulse lengths of the pulse pair in the waveform. The length of the waveform in samples varies between 460 and 690 samples. The received signal array has a length in the order of 1700 – 2600 samples. The consequence is lengthy calculations, which hampers quick analysis on various parameters. The PC used took about 16-24 hours for a single simulation run, but could, with its multi-core processor, run 8 simulations in parallel.

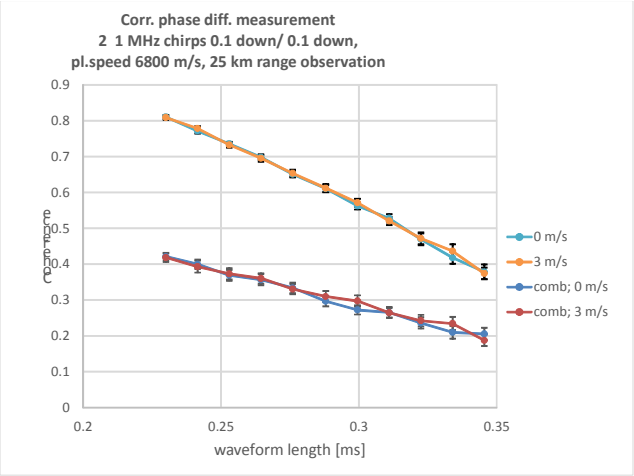

Figure 6: Coherence between the responses of the two pulses of a pulse pair after pulse compression, as a function of total wave form length. The chirped pulses prior to pulse compression have a length of 0.115 ms. The separation between the pulses runs from 0 to 0.11 ms.

A. Coherence estimation

The software was also used to estimate the coherence between the received signals from the two pulses in the pulse pair, as required for the Cramér-Rao bound calculation in eq. (1).

Fig. 6 shows a coherence estimation obtained from the simulations. In this case the pulse pair consisted of 2 down chirps of 0.115 ms, with separation varied between 0 and 0.11 ms. Simulations were run for ocean speeds of 0 and 3 m/s. The ocean speed does not noticeably influence the coherence. The 2 curves with the highest coherence are for the case of separation of the received signals from the pulses as already discussed, but this is not applicable in the DopSCA case. The lower two curves represent the combined response on the two pulses as it can be measured with SCA. They show a coherence gradually sinking with waveform length from 0.41 to 0.2. Note that in eq. (1) the increase in time between the pulses compensates for the decrease of the coherence with waveform length, resulting in almost no change of the measurement accuracy. As already indicated the best ocean LOS accuracy based on the coherence will be in the order of 0.6 m/s.

B. Phase difference due to scatterer ensemble motion

Fig. 7 shows a simulation result for the average phase in the cross correlation between the signals of the two pulses in the pulse pair. The forward looking (+45 deg) beam is used. Three plots are shown. The cross-correlation phase (which can be converted to ocean motion), the standard deviation on the cross-correlation phase, which represents the accuracy of the measurement and a comparison of simulated and theoretical phase difference between 0 and 3 m/s ocean current. In the gray areas results are included for waveform lengths longer than 0.3 ms, which is beyond the decorrelation time of the moving antenna, hence less meaningful results can be expected here.

In the left plot the cross-correlation phase for 0 and 3 m/s ocean current is displayed as a function of the waveform length. Essentially the delay between the two pulses of the pulse pair is varied from 0.116 ms, which is a nearly juxta-posted pulse pair case, to 0.23 ms. The phase for the 3 m/s current case decreases linearly with waveform length (up to 0.3 ms) as could be expected, whereas for 0 m/s the phase is nearly constant and close to zero. The error bars indicate the 95% confidence interval of each observation, which are based on the average of 64 runs x 16 looks = 1024 individual simulations. An individual observation is based on the cross-correlation between two range data series of 333 range samples (= 167 range resolution cells = 25 km).

In the plot also linear regression lines are drawn. Results in the gray areas are not taken into account in these regression lines. The 0 m/s regression line is particularly useful to find a precise offset value of the phase, which can increase the accuracy of the ocean motion measurement.

The plot in the middle shows the 16 look standard deviation (SD) on the cross-correlation phase observations as a function of the waveform length. The standard deviation is evaluated from 64 realizations. The 16 look values are particularly useful, as they relate closely to a 25 km travel length of SCA (which has 15 looks, see footnote 1), hence they indicate the expected accuracy for 25 x 25 km WVC.

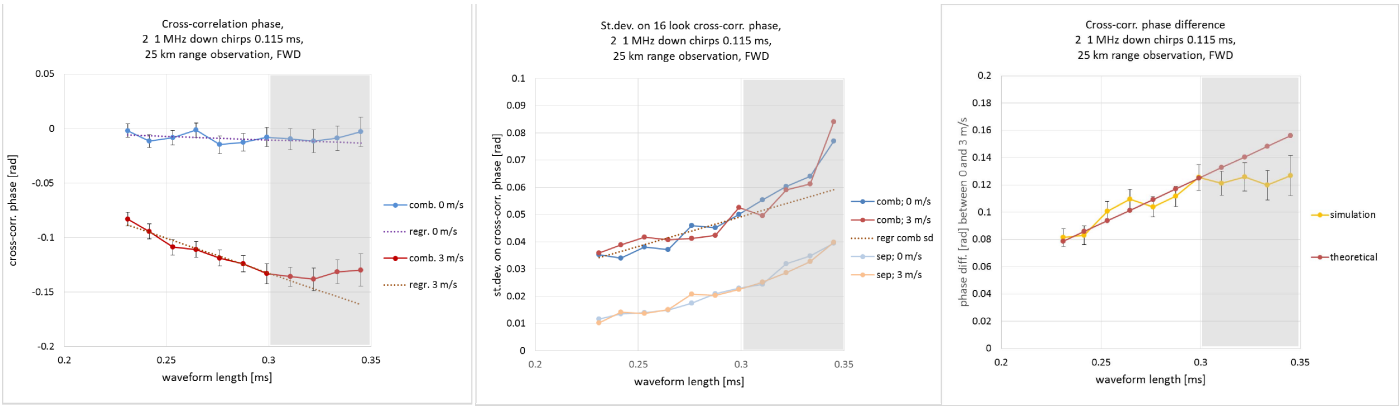

Figure 7: Numerical simulation result for a 0.115 msec pulse pair in the +45 deg beam.

Also shown are the SD's for received signals of the separated pulse responses, which is a theoretical case that cannot be achieved with the current radar configuration, as explained before. These SD values are much smaller, because there is no deterioration by the clutter of the other pulse.

The SD increases with waveform length, as can be expected, because the motion of the antenna leads to increasing decorrelation in the received signal with travel distance. Theoretically, at half an antenna length displacement, which occurs in approx. 0.235 ms, considerable decorrelation can be expected. However, the phase measurement leads to useful results up to approximately 0.3 ms.

The right plot shows the theoretical phase difference between 0 m/s and 3 m/s ocean current as a function of waveform length, along with the observed phase difference in simulations. These values are in good agreement up to 0.3 ms. In other simulations the linearity between the phase and the ocean current was confirmed.

C. *Measurement precision*

From the simulations the precision of the determined ocean current can be estimated. This is calculated by dividing the 16 look SD by the phase difference between 0 and 3 m/s and multiplication with 3 m/s. Table 2 displays the results. The column with results from the separate pulse responses (which again is not feasible with the SCA configuration) indicates that a high precision better than 0.5 m/s could be obtained for a 25 x 25 km WVC. The precision gradually decreases with waveform length.

Note that all precision values in table 2 indicate the 1 SD precision, meaning that 68% of the observations will fall in an interval of plus and minus the indicated value in table 2. This is the usual presentation of precision.

The third column indicates the precision that can be expected for the received signal from the SCA instrument, based on 0 m/s and 3 m/s measurements. Slightly better precision is obtained if the more accurate phase of the 0 m/s regression line is taken as reference (column 4). The precision is in the order of 1.1 m/s. This value is achievable with a measurement on a single WVC of 25 x 25 km. In this cell SCA can transmit 16 pulse pairs, if one of the extra pulses of the SCA is used, hence 16 looks. If the WVC resolution would be reduced to 50 x 50 km, then 4 times more looks can be accumulated, which brings the precision down to 0.55 m/s. This is in agreement with the 0.61 m/s value from the Cramér-Rao bound calculation (which was calculated for 15 looks). However this precision is in the radar range direction. The slant range to ground range projection of roughly 45 degrees results in a small deterioration by a factor 1.4. Still an accuracy below 1 m/s is expected. Note that theoretically, the accuracy for separate pulse responses for the 50 x 50 km WVCs could be in the order of 0.3 m/s.

Table 2: Measurement precision as function of waveform length for 25 x 25 km Wind Vector Cells.

measurement time	pulse responses separate (theoretical)	pulse responses combined	include regression line phase
in ms	precision in m/s	precision in m/s	precision in m/s
0.231	0.40	1.17	1.27
0.2415	0.54	1.54	1.36
0.253	0.40	1.09	1.15
0.2645	0.44	1.14	1.19
0.276	0.61	1.15	1.16
0.2875	0.54	1.10	1.04
0.299	0.56	1.19	1.17
0.3105	0.61	1.37	1.34
0.322	0.58	1.46	1.40
0.3335	0.65	1.37	1.42
0.345	0.75	2.09	2.17

VI. Conclusions

Obtaining ocean current information on scales of 50 km and smaller remains a challenge. In addition, Doppler measurements depend on waves, drifts and currents and accurate local wind information, such as from scatterometers, is necessary to obtain accurate currents. The purpose of this study is to investigate alternative ways to measure ocean current with the METOP SG wind scatterometer, after the studies in [4-6] turned out to be not feasible for several reasons. Care has been taken to come up with measurement strategies that can be applied on the SCA instrument without degrading or influencing other products of the mission. It is assumed that one or both extra pulses (which are normally foreseen for cross-pol measurements) are used. If both pulses are used (in the +45 and -45 deg. beams), it is even possible to determine ocean current direction in addition to speed.

SCA is not designed to measure small Doppler shifts and incur ocean currents from it. Therefore it cannot be expected that the quality of such measurements can fulfil the most stringent requirements of the oceanographic community. On the other hand, if it is possible without much effort to enhance the products of SCA with an ocean current product, than that is certainly valuable, even if other dedicated ocean current missions are under investigation.

The current study is far from complete, but shows promising results for a new and innovative way of measuring the ocean current vector. The precision found in simulations is well below 1 m/s for a 50 x 50 km WVC and is in line with theoretical expectation based on the Cramér-Rao bound.

A more detailed study is recommended, along with real system data testing. Many factors that influence the performance still require attention, e.g. the improvement of statistical reliability, platform attitude accuracy, realistic SNR inclusion in the simulation, better ocean surface models.

References

[1] Fabrice Ardhuin, et.al., 2018, Measuring currents, ice drift, and waves from space: the Sea Surface KInematics Multiscale monitoring (SKIM) concept, Ocean Sci 14:337-354, doi:10.5194/os-2017-65

[2] Chung-Chi Lin, et.al., 2012. EPS-SG Windscatterometer Concept Tradeoffs and Wind Retrieval Performance Assessment, IEEE Trans GRS, doi: 10.1109/TGRS.2011.2180393

[3] Dohan, K., and N. Maximenko, 2010. Monitoring ocean currents with satellite sensors, Oceanography 23(4):94–103, doi:10.5670/oceanog.2010.08.

[4] Fabry, P., et.al., 2013. Feasibility study of sea surface currents measurements with doppler scatterometers, ESA Living Planet Programme, 16/9/2013-20/9/2013, Edinburgh, UK, ESA.

[5] F. Fois, P. Hoogeboom, F. Le Chevalier and A. Stoffelen, 2015. DOPSCAT: A mission concept for a Doppler wind-scatterometer, 2015 IEEE International Geoscience and Remote Sensing Symposium (IGARSS), Milan, 2015, pp. 2572-2575, doi: 10.1109/IGARSS.2015.7326337.

[6] Franco Fois, 2015. Enhanced Ocean Scatterometry, PhD thesis, TU Delft, ISBN/EAN: 978-94-6259-883-6.

[7] P. R. Mahapatra and D. S. ZrniC, 1983. Practical Algorithms for Mean Velocity Estimation in Pulse Doppler Weather Radars Using a Small Number of Samples, IEEE Transactions on Geoscience and Remote Sensing, vol. GE-21, no. 4, pp. 491-501.

[8] Jose Marquez, Byron Richards, Christopher Buck, 2010. Wavemill: A Novel Instrument for Ocean Circulation Monitoring, 8th European Conference on Synthetic Aperture Radar, pp.1-3.

[9] Mouche Alexis, et.al., 2012. On the Use of Doppler Shift for Sea Surface Wind Retrieval From SAR, IEEE Transactions On Geoscience And Remote Sensing, 50(7), 2901-2909. Publisher's official version: http://doi.org/10.1109/TGRS.2011.2174998, Open Access version: http://archimer.ifremer.fr/doc/00088/19896/

[10] Frédéric Nouguier, et.al., 2018. Sea surface kinematics from near-nadir radar measurements, IEEE TGRS, doi: 10.1109/TGRS.2018.2833200.

[11] Phillips, O.M., 1977. The dynamics of the upper ocean (2nd ed.), Cambridge University Press. ISBN 0-521-29801-6, page 37, https://en.wikipedia.org/wiki/Stokes_drift#Example:_Deep_water_waves.

[12] Schulte, H.R., 2016. SCA Ocean Currents Measurement, Airbus report nr MOS-TN-ADSF-SCA-1000156094_V02.

[13] Scipal, K., 2017. Minutes of meeting on SCA Doppler review, ESA ref. nr. EOP-SM/3112.

[14] Raney, R.K., 1998. Radar Fundamentals: Technical Perspective, Chapter 2 in Principles and Applications of Imaging Radar, Manual of Remote Sensing, Third Edition, Volume 2, ASPRS, John Wiley and Sons Inc., Toronto.

[15] Rodríguez, Ernesto, et.al., 2018. Estimating Ocean Vector Winds and Currents Using a Ka-Band Pencil-Beam Doppler Scatterometer, Remote Sens. 10, no. 4: 576.

[16] James D. Taylor (ed.), 2016. Advanced Ultrawideband Radar: Signals, Targets, and Applications, CRC press.

[17] https://earth.esa.int/web/eoportal/satellite-missions/m/metop-sg.